Solvent−Solute Interactions Probed by Picosecond Time-Resolved Fluorescence Spectroscopy: Lifetime and Anisotropy Study of S_1 *trans*-4,4′-Diphenylstilbene

Xin Tan and Terry L. Gustafson*

Department of Chemistry, The Ohio State University, 100 West 18th Avenue, Columbus, Ohio 43210-1185

Received: September 22, 1999; In Final Form: March 1, 2000

Excited-state lifetimes and rotational reorientation times were obtained for *trans*-4,4′-diphenylstilbene (DPS) in a series of *n*-alkanes and nonalkane solvents as a function of temperature using picosecond time-resolved fluorescence lifetime and anisotropy measurements. The fluorescence lifetimes do not have a significant solvent or temperature dependence, indicating that isomerization via activated barrier crossing is not a dominant decay pathway for S_1 DPS. However, the temperature dependence of the lifetime is shown to be larger in polar solvents than nonpolar solvents. Arrhenius plots for polar solvents give two different decay channels in the low-temperature and high-temperature regions. The rotational reorientation time of DPS is sensitive to solvent environments. In a given solvent the rotational reorientation times depend linearly on η/T in agreement with the Debye−Stokes−Einstein theory. The data in *n*-alkane solvents show that the solute−solvent coupling, as evidenced by the friction coefficient, decreases as viscosity increases; in polar solvents, this trend appears to be reversed.

I. Introduction

A general approach for investigating solvent−solute interactions involves determining the rates of various chemical processes under different solvent conditions and associating the rates to bulk solvent properties. Time-resolved fluorescence spectroscopy is one of the primary tools for measuring the rates. Rotational relaxation measurements are sensitive to the solvent environment surrounding the reorienting molecule and have been used extensively to elucidate the fundamental nature of solvent−solute interactions.[1−8]

Our previous transient Raman and transient absorption experiments have demonstrated that *trans*-4,4′-diphenylstilbene (DPS) undergoes excited-state conformational changes and that the dynamics are solvent-dependent.[9,10] For this reason, DPS is an interesting probe molecule to investigate solvent−solute interactions. The present lifetime and reorientation study was undertaken to further the understanding of DPS photophysics and provide more information about solvation dynamics.

In this paper, we present the fluorescence lifetimes and rotational reorientation times of the first excited singlet state of DPS obtained from picosecond time-resolved fluorescence measurements in a variety of solvents over a range of temperatures. We observe that the emission rate constant exhibits little temperature dependence in most nonpolar solvents; the relatively larger temperature dependence in polar solvents reveals different high-temperature and low-temperature decay channels. The results are discussed in the context of fluorescence quantum yield, the barrier to isomerization, and the effects of viscosity, dielectric constant, and solvent structure. The rotational reorientation times can be reasonably well described by the modified Debye−Stokes−Einstein model. We find that the solute−solvent coupling in nonalkane solvents seems to correlate with solvent viscosity but differently in nonpolar and polar solvents. In the *n*-alkane series, the coupling is close to the slip boundary prediction and decreases as the chain size increases. We interpret the reorientation data in terms of solute−solvent and solvent−solvent interactions in the framework of rotational diffusion.

II. Experimental Section

Steady-State Spectroscopy. Steady-state absorption and emission spectra of DPS were obtained at room temperature. Absorption spectra were collected by a UV/vis spectrometer (Perkin-Elmer Lambda 20), and emission spectra were acquired from a fluorimeter (Jobin Yvon-Spex Instrument S. A., Inc., FluoroMax-2). Figure 1 shows the absorption and emission spectra of DPS in acetonitrile, from which the radiative rate constant of DPS was evaluated to be 7.1×10^8 s^{-1}.[11] Fluorescence quantum yields were calculated using 9,10-diphenylanthracene (DPA) of a known quantum yield about 0.83 as a standard reference, following the method of Berlman[12] and Birk.[11]

Time-Resolved Measurements. In the fluorescence lifetime and anisotropy experiments, pulses at 620 nm were generated by a cavity-dumped rhodamine 6G dye laser (Coherent, Inc., model 702-2, with a model 7220 cavity dumper), which was synchronously pumped by the second harmonic from a CW mode-locked Nd:YAG laser (Coherent, Inc., model Antares 76S). Cavity-dumped picosecond pulses at a repetition rate of 1 MHz were frequency-doubled (Spectra-Physics 390) to provide excitation at 310 nm. The excitation beam was sent through a UV polarization rotator to be rendered vertically polarized and was focused near the front surface of a 1.0 cm × 1.0 cm quartz sample cell by a 10 cm lens. The sample cell was placed inside a holder connected to a reservoir-type constant-temperature circulator (Fisher Scientific model 901).

The fluorescence emission was collected at 90°, passed through a polarization analyzer and a scrambler, focused into a subtractive−dispersive double monochromator (American Holographic DB-10S), and detected by a microchannel plate photomultiplier tube (MCP-PMT; Hammamatsu R-2809U-07).

* To whom correspondence should be addressed: 614-292-1832; gustafson.5@osu.edu.

10.1021/jp993389p CCC: $19.00
Published on Web 04/14/2000

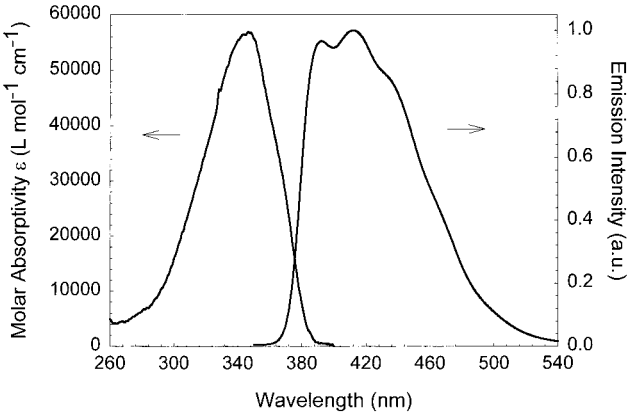

Figure 1. Absorption and fluorescence emission spectra of DPS in acetonitrile (10^{-6} M).

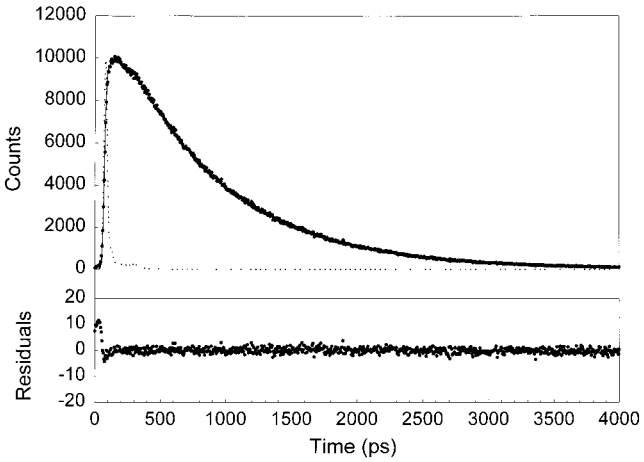

Figure 2. Typical IRF and fluorescence decay of DPS in acetonitrile at 50 °C. The dotted line is the IRF, and the points represent the experimental data of decay. The solid line through the points is the convolution of the IRF with a single-exponential model function having a decay constant of 775 ps. The residuals of the fit are shown with $\chi^2 = 1.991$.

Fluorescence decay profiles were acquired using the time-correlated single-photon-counting (TCSPC) method, with the time-to-amplitude converter (TAC; Tennelec TC-455) operated in reverse mode.[13] The MCP signal was sent through a Gigahertz preamplifier (EG&G Ortec 9306) to a picotiming discriminator (EG&G Ortec 9307) and served as the start pulse for TAC. The residual visible dye laser beam was sent into a fast photodiode and through a quad constant fraction discriminator (Tennelec TC-455) to provide the stop pulse. The TAC capacitance was transferred to a multichannel analyzer (Tennelec PCA-II), where the data were binned and displayed as histograms representing fluorescence decays. The instrument response was characterized by a full width at half-maximum (fwhm) of about 40 ps.

For the lifetime measurements, fluorescence decays were collected with the polarization analyzer set at magic angle (54.7°) with respect to the excitation polarization. Lifetimes were extracted from the decays via the method of iterative reconvolution using single-exponential model functions. Figure 2 shows a typical plot of the fluorescence decay of DPS in acetonitrile, the instrument response function, and a convoluted single-exponential decay fit to the data.

For the anisotropy measurements, fluorescence decays were collected separately with the polarization analyzer set parallel and then perpendicular to the UV excitation polarization. During collection the parallel and perpendicular polarized fluorescence decays were tail-matched in the region where the fluorescence

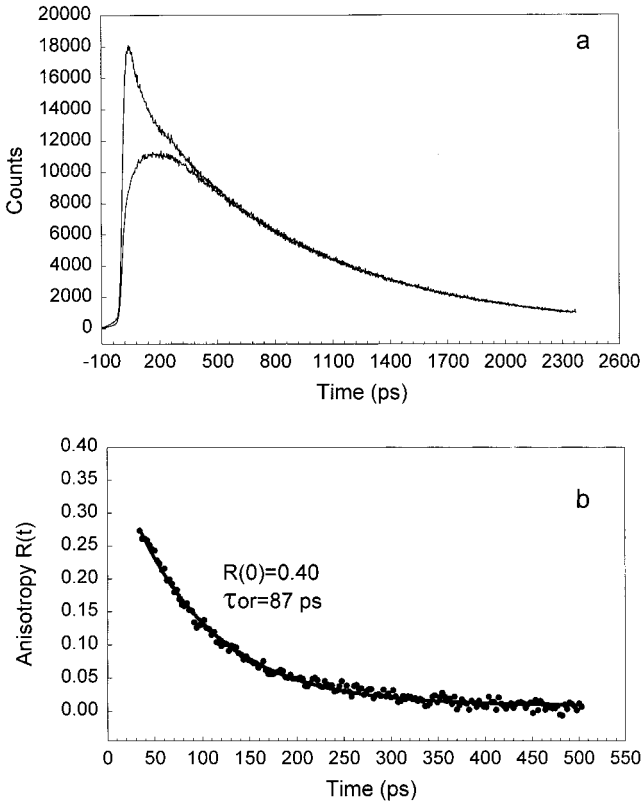

Figure 3. (a) Experimental fluorescence intensities, $I_{\parallel}$ (upper curve) and $I_{\perp}$ (lower curve) for DPS (about 10^{-6} M) in acetonitrile at 25 °C. (b) The points are experimental values of time-dependent fluorescence anisotropy from data in (a) by eq 2. The solid line is the best single-exponential fit with a time constant of 87 ps for the anisotropy decay.

depolarization was essentially complete. From the decays the induced orientational anisotropy was calculated and fit to an exponential function from which the rotational reorientation time and the initial anisotropy were obtained, as shown in Figure 3.

Chemicals. *trans*-4,4′ diphenylstilbene (DPS) and 9,10-diphenylanthracene (DPA) of 99% purity were purchased from Lancaster. Spectrophotometric grade acetonitrile, *N*,*N*′-dimethylformamide, dichloromethane, cyclohexane, benzene, dioxane, octane, decane, dodecane, and tetradecane were obtained from Aldrich Chemical Co. and used without further purification. The solutions were prepared around 10^{-6} M and argon-purged, magnetically stirred, and changed frequently during experiments. The temperature of the sample was controlled for each time-resolved measurement in the range of −10 to 85 °C.

III. Results

Fluorescence Quantum Yields. Steady-state absorption and emission spectra of DPS at room temperature show little solvent dependence of peak positions and Stokes shifts (variations within 5 nm). The fluorescence quantum yields of DPS at room temperature were measured to be 0.73 in dichloromethane, 0.66 in benzene, 0.74 in dioxane, 0.72 in acetonitrile, 0.72 in *N*,*N*′-dimethylformamide, 0.80 in cyclohexane, 0.69 in octane, 0.72 in decane, 0.72 in deodecane, and 0.73 in tetradecane.

Fluorescence Lifetimes. In the fluorescence lifetime measurements, all fluorescence decays could be adequately fit by the convolution of single-exponential model functions with the instrument response. Table 1 lists the fluorescence lifetime data of DPS. We note that the fluorescence lifetime data do not exhibit strong temperature or solvent dependence except in the polar solvents acetonitrile and *N*,*N*′-dimethylformamide. Ar-

TABLE 1: Fluorescence Lifetimes, τ_f[a] of DPS in All Solvents and at Various Temperatures

	temp, °C								
solvent	−10	0	10	20	30	40	50	60	70
acetonitrile	916	920	900	883	850	818	773	729	676
N,*N*′-dimethylformamide	900	895	890	884	881	870	850	818	775
benzene			835	833	832	828	821	803	794
cyclohexane			859	848	852	856	848	840	831
dichloromethane	879	875	871	873	859				
dioxane				900	897	890	882	869	841
octane	871	863	868	862	860	851	850	843	822
decane	881	878	881	880	876	869	862	857	853
dodecane		888	880	889	882	882	875	866	851
tetradecane			896	893	895	887	887	865	865

[a] Uncertainties in the measurements are within 2% of the lifetime values.

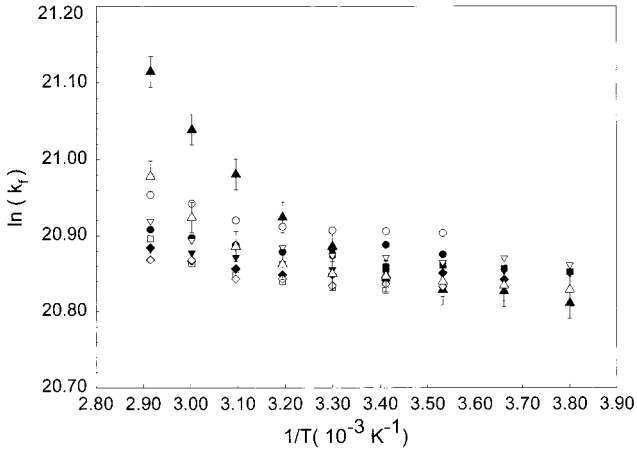

Figure 4. Arrhenius plots of DPS emission in all solvents: (▲) acetonitrile, (△) *N*,*N*′-dimethylformamide, (■) dichloromethane, (●) cyclohexane, (○) benzene, (□) dioxane, (▽) octane, (▼) decane, (◆) dodecane, and (◇) teradecane.

rhenius plots of the experimentally determined rate constants are shown in Figure 4. The results in acetonitrile and *N*,*N*′-dimethylformamide demonstrate dual-slope behavior in the high-temperature region (30−70 °C) and the low-temperature region (−10−30 °C) where the emission rate is almost constant. On the basis of previous studies of stilbene and its derivatives, we suggest that isomerization is the activated process giving rise to the temperature dependence in the high-temperature region.[14] Figure 5 shows the Arrhenius plots of DPS isomerization in the high-temperature region, the isomerization rate is calculated by subtracting the low-temperature rate constant from the high-temperature emission rate, and the solid and dash−dotted lines are the least-squares fits of the data in acetonitrile and *N*,*N*′-dimethylformamide, respectively, to the linearized Arrhenius law

$$\ln k_{ISO} = \ln A - E_a/RT \qquad (1)$$

where k_{ISO} is the isomerization rate constant, A is the preexponential frequency factor, E_a is the activation barrier, R is the ideal gas constant, and T is the temperature. The activation barrier to isomerization is 9.8 ± 0.5 kcal/mol K in acetonitrile and 13.9 ± 0.4 kcal/mol K in *N*,*N*′-dimethylformamide.

Rotational Reorientation. The parallel polarized fluorescence decay $I_{||}(t)$ and perpendicular polarized fluorescence decay $I_{\perp}(t)$ were measured independently, and the induced orientational anisotropy function used in characterizing the probe molecule dynamic behavior was given by

$$R(t) = \{I_{||}(t) - I_{\perp}(t)\}/\{I_{||}(t) + 2I_{\perp}(t)\} \qquad (2)$$

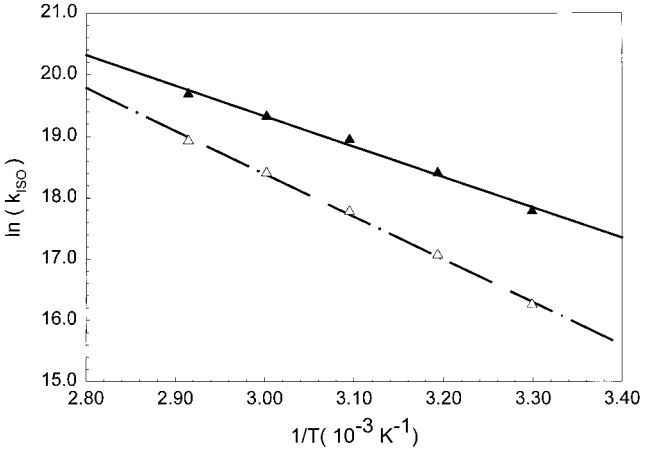

Figure 5. Arrhenius plots of DPS isomerization in polar solvents in the high-temperature region (30−70 °C): (▲) acetonitrile, (△) *N*,*N*′-dimethylformamide. The solid and dash−dotted lines are the linear Arrhenius fits.

The rotational reorientation time τ_{or} and initial anisotropy R(0) were calculated by nonlinear regression of the function $R(t)$ vs time; the anisotropy decays in all solvents were well-described by a single-exponential decay with a small offset. The rotational reorientation times and initial anisotropy values for DPS in some of the solvents used for the experiments and at various temperatures are presented in Table 2.[15]

Rotational reorientation in a wide variety of solvent−solute systems can be approximated by the modified Debye−Stokes−Einstein (DSE) equation.[1,3]

$$\tau_{or} = \eta VF/kTS \qquad (3)$$

where η is the solvent bulk viscosity, V is the probe molecule hydrodynamic volume, k is the Boltzmann constant, T is the temperature, S is a shape factor to account for nonspherical probe molecular shape as calculated from Perrin's equations,[16,17] and F is a friction coefficient, equal to 1 for the stick boundary condition and <1 for the slip boundary condition with its exact value depending on the probe molecular shape.[17,18]

The probe molecule DPS was modeled as a prolate ellipsoid with its transition dipole lying along the long symmetry axis, in agreement with the experimental data of exclusive single-exponential anisotropy decays with initial anisotropy values around 0.4. The hydrodynamic volume of DPS was calculated to be 317 Å^3 by the method of van der Waals increments.[19] The prolate axial ratio for DPS, the ratio of the long to the short symmetry axis, was 4.65 after geometry optimization using the PM3 semiempirical method. These results calculate the shape factor S to be 0.239 and the slip friction coefficient to be 0.637.[17] With the above quantities computed, the rotational reorientation times of DPS under the stick and slip boundary conditions were represented by τ_{or} (stick) = 96.22 (η/T) and τ_{or} (slip) = 61.29 (η/T), τ_{or} in units of ps and (η/T) in units of 10^{-3} cP K^{-1}. Figures 6 and 7 are plots of τ_{or} vs. η/T for all the solvents with the dashed line referring to the slip boundary and the solid line to the stick boundary.

Several observations can be made from Figures 6 and 7. First, in each solvent, the rotational reorientation time exhibits an approximate linear dependence upon η/T, and the slope tends to vary with different solvents. Second, the rotational reorientation times are closer to the slip boundary condition for the linear alkanes than the nonalkane solvents and are even below the slip predictions (subslip) in the larger alkanes at low temperatures.

TABLE 2: Experimental Initial Anisotropy Values and Rotational Reorientation Times for DPS in Various Solvents at Different Temperatures

solvent	temp, °C	η, cP	$R(0)$	τ_{or}, ps
acetonitrile	−4.0	0.495	0.393 ± 0.008	132 ± 4
	4.0	0.452	0.394 ± 0.017	118 ± 5
	13.0	0.409	0.407 ± 0.011	109 ± 3
	25.0	0.360	0.403 ± 0.011	87 ± 3
	37.0	0.320	0.400 ± 0.013	76 ± 2
	45.0	0.297	0.394 ± 0.012	72 ± 2
	53.0	0.276	0.404 ± 0.020	65 ± 3
	66.0	0.248	0.401 ± 0.026	59 ± 3
cyclohexane	8	1.200	0.381 ± 0.006	269 ± 7
	13.0	1.094	0.389 ± 0.006	246 ± 6
	18.0	1.006	0.368 ± 0.009	229 ± 9
	26.0	0.881	0.378 ± 0.011	196 ± 10
	33.0	0.789	0.400 ± 0.009	163 ± 6
	37.0	0.741	0.401 ± 0.008	158 ± 4
	42.0	0.690	0.399 ± 0.011	142 ± 5
	45.0	0.660	0.390 ± 0.009	134 ± 4
	52.0	0.600	0.407 ± 0.006	113 ± 3
	61.0	0.532	0.408 ± 0.010	106 ± 4
	66.0	0.498	0.391 ± 0.010	100 ± 3
dichloromethane	−4.0	0.558	0.400 ± 0.009	175 ± 5
	4.0	0.510	0.398 ± 0.010	153 ± 4
	13.0	0.464	0.397 ± 0.012	138 ± 4
	25.0	0.413	0.393 ± 0.010	115 ± 4
	37.0	0.371	0.413 ± 0.018	95 ± 4
octane	3.0	0.672	0.393 ± 0.009	171 ± 6
	8.0	0.629	0.395 ± 0.008	154 ± 5
	19.0	0.547	0.409 ± 0.010	128 ± 4
	29.0	0.485	0.411 ± 0.009	114 ± 3
	40.0	0.428	0.407 ± 0.012	97 ± 3
	51.0	0.381	0.409 ± 0.015	85 ± 3
	61.0	0.344	0.398 ± 0.013	63 ± 3
	72.0	0.310	0.418 ± 0.016	59 ± 3
tetradecane	8.0	3.096	0.389 ± 0.005	554 ± 11
	14.0	2.673	0.392 ± 0.006	485 ± 11
	19.0	2.383	0.380 ± 0.008	440 ± 14
	25.0	2.101	0.398 ± 0.008	380 ± 10
	30.0	1.893	0.390 ± 0.007	336 ± 9
	42.0	1.513	0.404 ± 0.010	266 ± 8
	52.0	1.281	0.400 ± 0.007	206 ± 6
	62.0	1.103	0.396 ± 0.008	180 ± 5
	71.0	0.968	0.385 ± 0.016	151 ± 10
	82.0	0.844	0.404 ± 0.012	131 ± 5

IV. Discussion

Fluorescence Lifetime. Compared with *trans*-stilbene[20−23] and the diphenylpolyenes,[24−29] DPS has a much higher fluorescence quantum yield (∼0.7) as shown from the steady-state measurements at room temperature. The fluorescence lifetime data in Table 1 also demonstrate less significant temperature and solvent dependence. These data imply that photoisomerization via activated barrier crossing is not an important decay pathway for the DPS excited state.

Among all the solvents tested, the temperature dependence of the fluorescence lifetime is greater in polar solvents than nonpolar solvents. The maximum change in lifetime with temperature is about 25% in acetonitrile and 13% in *N*,*N*′-dimethylformamide but less than 6% in the remaining nonpolar solvents. For polar solvents such as acetonitrile and *N*,*N*′-dimethylformamide, which have the same value for the dielectric constant, the temperature dependence is larger in acetonitrile, the solvent with a lower viscosity and smaller molecular volume. Even though it is difficult to derive an exact correlation of the observed rate constant changes with solvent properties, we suggest the following possible contributions of viscosity and dielectric constant to the nonradiative isomerization process

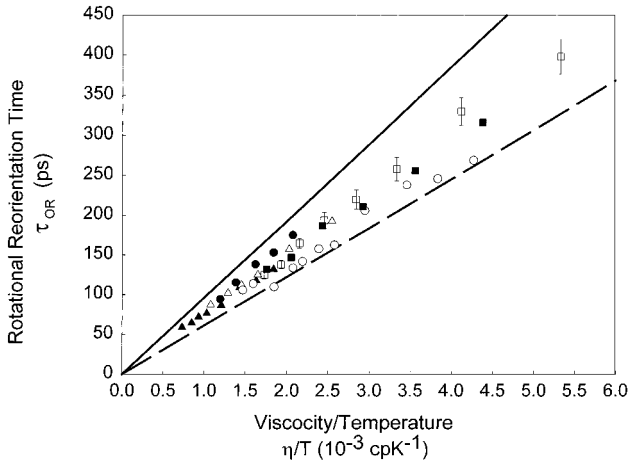

Figure 6. Plots of rotational reorientation time τ_{OR} vs the viscosity over temperature η/T for DPS in (▲) acetonitrile, (△) benzene, (○) cyclohexane, (●) dichloromethane, (■) dioxane, and (□) *N*,*N*′-dimethylformamide. The largest error bars from the fit uncertainty of the anisotropic fluorescence decay curves are shown. The dashed line represents τ_{OR} predicted with slip boundary parameter, while the solid line represents τ_{OR} predicted with stick boundary parameter as explained in the paper.

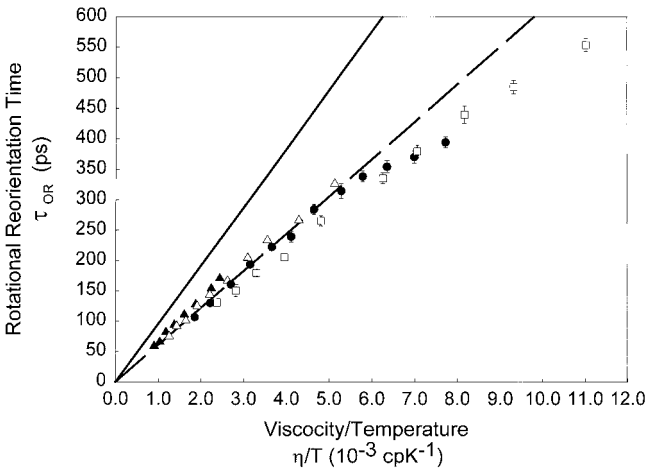

Figure 7. Plots of rotational reorientation time τ_{OR} vs the viscosity over temperature η/T for DPS in linear alkane solvents: (▲) octane, (△) decane, (●) dodecane, and (□) tetradecane. The largest error bars from the fit uncertainty of the anisotropic fluorescence decay curves are shown. The dashed line represents τ_{OR} predicted with slip boundary parameter, while the solid line represents τ_{OR} predicted with stick boundary parameter.

based on our experimental results. We consider the twisted state of DPS to be more polar than the initial excited state and better solvated in polar solvents. Thus the high dielectric constant of polar solvents can reduce the activation barrier by stabilizing the DPS excited state, favoring the conformational changes associated with the isomerization process. High solvent viscosity can impose larger friction on the solute and increase the activation energy to isomerization. Previous isomerization studies of *trans*-stilbene[30]and diphenylbutadiene[26] have also demonstrated such solvent effects on the activation energy in solution.

The Arrhenius plots of DPS emission rates in acetonitrile and *N*,*N*′-dimethylformamide reveal the presence of two decay channels, one of which dominates at high temperatures (30−70 °C), the other at low temperatures (−10−30 °C). In the low-temperature decay channel, the fluorescence lifetimes tend to be independent of temperature or increase slightly with decreasing temperature. Similar results have been shown for diphen-

TABLE 3: Linear Regression Fits of DPS Rotational Reorientation Times as a Function of (η/T) for Each Solvent

solvent	slope A 10^3 K ps/cP	intercept B, ps	friction coefficient F	viscosity (25 °C), cP	dielectric constant
N,*N*′-dimethylformamide	81.9 ± 4.3	−15.9 ± 9.7	0.851	0.794	36.7(25 °C)
acetonitrile	68.1 ± 3.4	8.0 ± 4.0	0.707	0.369	36.7(25 °C)
dichloromethane	90.5 ± 6.3	11.5 ± 10.1	0.941	0.413	9.08(25 °C)
benzene	72.1 ± 3.5	8.5 ± 5.4	0.749	0.604	2.274(25 °C)
dioxane	70.1 ± 3.1	7.8 ± 7.8	0.728	1.177	2.209(25 °C)
cyclohexane	62.8 ± 1.9	4.1 ± 4.2	0.653	0.894	2.016(25 °C)
octane	73.1 ± 2.8	−5.9 ± 4.1	0.760	0.508	1.948(20 °C)
decane	64.4 ± 1.3	0.8 ± 2.8	0.669	0.838	1.991(20 °C)
dodecane (>15 °C)	59.7 ± 1.8	3.8 ± 5.4	0.620	1.383	2.014(20 °C)
tetradecane	50.8 ± 1.0	12.0 ± 5.1	0.528	2.128	

ylbutadiene in hexane at low temperatures.[26] We suggest that the high solvent viscosities at low temperatures impede the large amplitude motion of DPS, minimizing the isomerization yield consistent with previous results on substituted stilbenes.[14] The average lifetime for the low-temperature channel is about 890ps, and the nonradiative rate constant is calculated to be 4.1×10^8 s^{-1}, which could be attributed to intersystem crossing and internal conversion.[26,30] Assuming that the intrinsic nonradiative processes of intersystem crossing and internal conversion are not temperature-dependent,[11,31] we can estimate the isomerization rates at high temperatures using $k_{ISO} = k_f - k_r - (k_{ISC} + k_{IC})$. The emission rate k_f can be calculated from the fluorescence lifetime data, the radiative rate constant k_r is 7.1×10^8 s^{-1}, and the combined intersystem crossing and internal conversion rate constants ($k_{ISC} + k_{IC}$) can be approximated by the nonradiative rate constant derived from the low-temperature channel. Figure 5 shows the linear Arrhenius fittings for the high-temperature decay channel. The activation barrier is lower in acetonitrile than *N*,*N*′-dimethylformamide, which demonstrates that for solvents of similar polarity, lower viscosity correlates with lower activation energy to isomerization.

Rotational Reorientation. According to the geometry optimization of DPS, the moment of inertia I is 377.2 amu Å^2; therefore, the free-rotor time $\tau_0 = (2\pi/9)(I/kT)^{1/2}$ over the experimental temperature range is approximately 1 ps.[17] For the values in Table 2, the ratio of the rotational reorientation time over the free-rotor time τ_{or}/τ_0 is in the range of 60−600 $\gg 1$, and this confirms the diffusional rather than inertial nature of the molecular reorientation and validates using the DSE model of rotational diffusion.

The friction coefficient F in the DSE model for DPS is 1.0 for the stick boundary and 0.637 for the slip boundary. The data in Figures 6 and 7 are fit to $\tau_{or} = A(\eta/T) + B$. The friction coefficient F can be calculated from slope A. Table 3 provides the results of the linear regression fittings along with the viscosity and dielectric constant for each solvent. From Table 3, we can observe that there seems to be two opposite kinds of correlation between the friction coefficient and the solvent viscosity: in nonpolar solvents (dielectric constant < 15), the friction coefficient in general decreases as solvent viscosity increases; in polar solvents (acetonitrile and *N*,*N*′-dimethylformamide), the friction coefficient increases with higher viscosity. Furthermore, the slope of the least-squares fits decreases along the alkane series, varying by less than a factor of 1.5 from octane to tetradecane. The friction coefficient F decreases from 0.760 above the slip boundary for octane to 0.528 below the slip boundary for tetradecane. These data suggest that, as solvent size increases for a similar type of solvent, the solute−solvent coupling gets weaker.[21,22,32] As the number of polar and nonpolar solvents being tested in the experiments is quite limited, it is difficult to isolate the effects of solvent viscosity, size, and polarity and draw definite conclusions on the correlation between the friction coefficient and the solvent properties. The solvent-independent results of the steady-state absorption and emission spectra of DPS at room temperature imply no effects of complex solvent structure on solvent−solute interactions.[1,17]

V. Conclusion

We have investigated the excited-state lifetimes and the reorientational behavior of DPS in a variety of solvents using picosecond time-resolved fluorescence spectroscopic methods. Fluorescence lifetimes of DPS show much less solvent and temperature dependence compared with *trans*-stilbene and the diphenylpolyenes, which implies that there is a significant barrier to isomerization and that isomerization is not a major decay pathway for the DPS excited state. The temperature dependence of the lifetimes is shown to be larger in polar solvents than nonpolar ones; Arrhenius plots reveal a low-temperature decay channel with almost no temperature dependence and a high-temperature decay channel with larger temperature dependence. We suggest that dielectric stabilization of S_1 DPS in polar solvents reduces the activation barrier to isomerization, and higher solvent viscosity increases the activation energy. Further examination of DPS in supercritical fluids with a wide range of variations in solvent polarity and viscosity may provide insight into possible functional dependence of the isomerization barrier height on the solvent viscosity and dielectric constant.

The rotational reorientation times vary linearly with η/T in accord with the modified Debye−Stokes−Einstein equation. Solute−solvent coupling represented by the friction coefficient in nonpolar solvents tends to decrease as viscosity increases, and the opposite trend seems to be shown in polar solvents, which is not conclusive owing to the limited number of polar solvents tested. The data in linear alkanes also demonstrate decreasing coupling with increasing solvent size.[21,22,32]

We want to emphasize the intrinsically different information about solvation dynamics probed by time-resolved fluorescence and transient Raman spectroscopy.[9,10] Time-resolved fluorescence spectroscopy gives information through reaction rate changes in differing solvent conditions, while transient Raman provides microscopic details about solvent−solute interactions through mode-specific vibrational structural changes. Combined analyses are critical for sorting out the relative contributions of solvent viscosity, dielectric constant, and solvent structure to solvation dynamics.

Acknowledgment. We thank Claudia Turro for generously providing us access to her fluorimeter in obtaining the steady-state emission spectra.

References and Notes

(1) Blanchard, G. J. *J. Phys. Chem.* **1988**, *92*, 6303−6307.
(2) Blanchard, G. J. *J. Phys. Chem.* **1991**, *95*, 5293−5299.
(3) Blanchard, G. J.; Cihal, C. A. *J. Phys. Chem.* **1988**, *92*, 5950−5954.
(4) Blanchard, G. J. *J. Chem. Phys.* **1987**, *87*, 6802−6808.

(5) Jiang, Y.; Blanchard, G. J. *J. Phys. Chem.* **1994**, *98*, 6436−6440.
(6) Jiang, Y.; Blanchard, G. J. *J. Phys. Chem.* **1995**, *99*, 7904−7912.
(7) Rasimas, J. P.; Blanchard, G. J. *J. Phys. Chem.* **1995**, *99*, 11333−11338.
(8) Jas G. S.; Wang Y.; Pauls S. W.; Johnson C. K.; Kuczera K. *J. Chem. Phys.* **1997**, *107*, 8800−8812.
(9) Butler, R. M.; Lynn, M. A.; Gustafson, T. L. *J. Phys. Chem.* **1993**, *97*, 2609−2617.
(10) Leonard, J. D.; Gustafson, T. L. *J. Raman Specstrosc.* **1999**.
(11) Birks, J. B. *Photophysics of Aromatic Molecules*, 1st ed.; John Wiley & Sons: New York, 1970; pp 166−170.
(12) Berlman, I. B. *Handbook of Fluorescence Spectra of Aromatic Molecules*, second ed.; Academic Press: New York, 1971.
(13) O'Connor, D. V.; Phillips, D. *Time-correlated single photon counting*; Academic Press, Inc.: London, 1984.
(14) Sun, Y. P.; Saltiel, J.; Park, N. S.; Hoburg, E. A.; Waldeck, D. H. *J. Phys. Chem.* **1991**, *95*, 10336−10344.
(15) VisWanath, D. S.; Natarajan, G. *Data Book on the Viscosity of Liquids*; Hemisphere Publishing Corp.: New York, 1989.
(16) Perrin, F. *J. Phys. Radium* **1934**, *5*, 497−511.
(17) Fleming, G. R. *Chemical Applications of Ultrafast Spectroscopy*, 1st ed.; Oxford University Press: New York, 1986.
(18) Hu, C.-M.; Zwanzig, R. J. *J. Chem. Phys.* **1974**, *60*, 4354−4357.
(19) Edward, J. T. *J. Chem. Educ.* **1970**, *47*, 261−270.
(20) Courtney, S. H.; Fleming, G. R. *J. Chem. Phys.* **1985**, *83*, 215−222.
(21) Courtney, S. H.; Kim, S. K.; Canonica, S.; Fleming, G. R. *J. Chem. Soc., Faraday Trans. 2* **1986**, *82*, 2065−2072.
(22) Kim, S. K.; Fleming, G. R. *J. Phys. Chem.* **1988**, *92*, 2168−2172.
(23) Weaver, W. L.; Huston, L. A.; Iwata, K.; Gustafson, T. L. *J. Phys. Chem.* **1992**, *96*, 8956−8961.
(24) Fleming, G. R.; Velsko, S. P.; Waldeck, D. H. *Springer Ser. Chem. Phys.* **1982**, *23*, 238−241.
(25) Fleming, G. R.; Waldeck, D. H.; Keery, K. M.; Velsko, S. P. *NATO ASI Ser., Ser. C* **1984**, *127*, 67−77.
(26) Velsko, S. P.; Fleming, G. R. *J. Chem. Phys.* **1982**, *76*, 3553−3562.
(27) Keery, K. M.; Fleming, G. R. *Chem. Phys. Lett.* **1982**, *93*, 322−326.
(28) Anderton, R. M.; Kauffman, J. F. *J. Phys. Chem.* **1995**, *99*, 14628−14631.
(29) Anderton, R. M.; Kauffman, J. F. *J. Phys. Chem.* **1994**, *98*, 12117−12124.
(30) Brey, L. A.; Schuster, G. B.; Drickamer, H. G. *J. Chem. Phys.* **1979**, *71*, 2765−2772.
(31) Birks, J. B. *Organic Molecular Photophysics*, John Wiley & Sons: London, 1975.
(32) Waldeck, D. H.; Fleming, G. R. *J. Phys. Chem.* **1981**, *85*, 2614−2617.